NGU Report 2001.027

Multispectral Remote Sensing of Caliche in Chile and Namibia: feasibility study

NGU Norges geologiske undersøkelse
Geological Survey of Norway
N-7491 Trondheim, Norway

REPORT

Report no.: 2001.027	ISSN 0800-3416	Grading: ~~Confidential until 2006~~ åpen

Title:

Multispectral Remote Sensing of Caliche in Chile and Namibia: feasibility study

Authors:	Client:
John F. Dehls	Norsk Hydro
County:	Commune:
Map-sheet name (M=1:250.000)	Map-sheet no. and -name (M=1:50.000)
Deposit name and grid-reference:	Number of pages: 22 Price (NOK): Map enclosures:

Fieldwork carried out:	Date of report:	Project no.:	Person responsible:
	22.03.2001	291600	Dyrkin Nordgulen

Summary:

Nitrate deposits in the Atacama Desert of northern Chile have been mined for more than a century and a half. Preservation of these areas of *caliche* has been due to the hyper-arid climate. The Namib Desert in Namibia has many similarities to the Atacama Desert. This study examines the feasibility of using satellite images to identify likely areas of nitrate.

The new ASTER instrument onboard NASA's Terra satellite has a unique combination of high resolution and good spectral resolution in the visible to thermal infrared spectrum. A set of scenes acquired in October 2000 has been analysed using statistical methods. Unique spectral classes identified in the image show a spatial correlation with areas of known nitrate deposits.

Further work must include the acquisition of atmospherically corrected data, samples of surficial materials for laboratory measurement, field-based measurement of spectra, and comparison with known geology.

Keywords: Nitrate	Remote Sensing	Infrared
Chile	Namibia	

CONTENTS

FIGURES

PLATES

1. Introduction

The nitrate deposits in the Atacama Desert of northern Chile have been mined for more than a century and a half. Highly soluble salts that have accumulated in permeable regolith and fractured bedrock have been preserved due to the hyper-arid climate. These deposits are known as *caliche*. The origin of the deposits remains speculative to this day. One likely explanation is summarized in Ericksen (1983). During the late Tertiary and Quaternary periods, increased rainfall resulted in widespread playa lakes in the Atacama Desert. Nitrate deposits formed by direct crystallization during evaporation. Saline material may have come from sea salts, carried inland in fog droplets (Ericksen 1983). The source of the nitrate may have been nitrogen fixation and nitrification of ammonium by algae and bacteria in the lakes. It may also be atmospheric deposition (Böhlke et al. 1997). The nitrates have since been reworked by wind and water.

While the conditions for the formation of nitrate deposits in Chile may not have been unique, the long-term hyper-arid conditions necessary to their preservation are very rare. One exception may be the Namib Desert, along the Skeleton Coast of Namibia, where years can go by without rainfall. Many parallels can be drawn between the Namib and Atacama deserts. Both are found along the west coast of a continent between about 19°S and 26°S. Both have a cold ocean current (the Humbolt along Chile and the Benguela along Namibia) that leads to abundant fog. Both have been arid since at least mid-Miocene time. The similarities suggest that the Namib Desert may be a good exploration target for nitrate deposits.

The size of the Namib Desert area rules out a ground-based exploration survey without first identifying specific targets. The goal of the current study is to assess the feasibility of using satellite images to identify likely areas of nitrate. By studying known deposits in Chile, it is hoped that characteristic spectral features will be found that can then be used to identify areas of caliche formation in Namibia.

2. Theory

Within the visible, near and shortwave infrared wavelengths, materials reflect solar energy in various quantities depending on wavelength. *Reflectance* is the ratio of the energy reflected by a material to that incident upon it. Satellite sensors measure the amount of reflected solar radiation from a given area. Within the thermal infrared wavelengths, satellite sensors measure energy emitted from a given area. The amount of energy measured is a function of both the temperature of the area and the efficiency at which the material emits energy. *Emissivity* is the ratio of the emitted energy from a material to that from a blackbody at the same temperature.

Many varieties of vegetation, soil and rocks can be distinguished from one another by their characteristic patterns of reflectance, or *spectra* within the visible to shortwave wavelengths. These spectra can be measured in the field with portable instruments, or in the laboratory. Collections of thousands of these spectra exist and can be used as reference when interpreting unknown spectra. Recently it has been found that many materials that do not exhibit unique spectral features within the shortwave wavelengths have characteristic features within the thermal wavelengths.

For several decades, the Landsat satellites have been the workhorses of the geological remote sensing community. They have captured images of the entire earth countless times, and the

combination of visible and shortwave bands has been used to distinguish variations in rock type, alteration, and structural features. This last ability has been enhanced with Landsat 7 by the addition of a panchromatic (0.52-0.9 μm) band with a 15 metre resolution. In December 1999, NASA launched a new satellite called Terra, as part of its Earth Observing System (EOS). Along with several other instruments, Terra carries an imaging instrument called ASTER (Advanced Spaceborne Thermal Emission and Reflection Radiometer).

The new ASTER instrument is particularly suited to geological studies. It has three bands within the visible to near infrared wavelengths, all with 15 metre resolution. Where Landsat has two bands within the shortwave wavelengths, ASTER has six, allowing much more precise identification of diagnostic spectra. In addition, ASTER has five bands within the thermal infrared wavelengths. Table 1 shows a comparison between Landsat and ASTER.

Table 1 Comparison of spectral range and resolution of Landsat TM and ASTER instruments. The Landsat 7 ETM instrument has an additional panchromatic band with a 15 metre resolution and a spectral range between 0.52 and 0.9 μm.

	ASTER band	Spectral range (μm)	Resolution (metres)	Landsat band	Spectral range (μm)	Resolution (metres)
VNIR (visible to near infrared)	no data			1	0.45-0.52	30
	1	0.52-0.60	15	2	0.52-0.60	30
	2	0.63-0.69	15	3	0.63-0.69	30
	3	0.76 0.86	15	4	0.76-0.90	30
SWIR (shortwave infrared)	4	1.60-1.70	30	5	1.55-1.75	30
	5	2.145-2.185	30	7	2.08 -2.35	30
	6	2.185-2.225	30			
	7	2.235-2.285	30	no data		
	8	2.295-2.365	30			
	9	2.360-2.430	30			
TIR (thermal infrared)	10	8.125-8.475	90			
	11	8.475-8.825	90			
	12	8.925-9.275	90			
	13	10.25-10.95	90	6	10.4 -12.5	60
	14	10.95-11.65	90			

2.1 Data Processing

2.1.1 Atmospheric correction

As of January 2001, ASTER data available was of the type 'Level 1B: Registered radiance at the sensor.' This data has been geometrically corrected to remove effects of satellite motion, earth curvature and so on. The values in the data reflect the amount of energy reaching the satellite. In order to determine the reflectance values for the individual pixels, the data must be atmospherically corrected. In other words, the scattering and absorbing properties of the atmosphere must be determined and corrected for, as well as the angle between the sun and the surface. Atmospheric correction requires an input model of the atmosphere at the time of the image acquisition. Such a model can be derived from low-resolution data from the MODIS instrument, also onboard the Terra satellite. Atmospherically corrected data were not yet available from NASA at the beginning of this project, but are available now.

2.1.2 Calculation of emissivity from thermal bands

Once atmospheric corrections have been applied to ASTER thermal infrared data, the resulting radiance-from-source information must be further processed to separate surface temperatures from emissivity. There are a number of methods available to separate these values (Hook et al. 1992). NASA plans to have separate temperature and emissivity data products available within the next few months. Current software available at NGU is capable of doing the separation, but only if atmospherically corrected input data is available. Atmospherically corrected TIR data is not yet available.

2.1.3 Identification of surface materials in images (classification)

There are a number of standard techniques available to separate digital images into various classes. Unsupervised classification is an iterative procedure whereby the image pixels are subdivided into a number of clusters or classes. The Isodata technique used for this study calculates class means evenly distributed in the data space and then iteratively clusters the remaining pixels using minimum distance techniques. Each iteration recalculates means for each class and reclassifies pixels with respect to the new means. This process continues until the number of pixels in each class changes by less than a selected threshold, in this case 2%. The advantage of an unsupervised technique is that no a priori information is necessary.

Supervised classification involves the identification of training regions, where the pixels belong to a known class. The rest of the pixels in the image are then classified as belonging to one of the known classes and assigned a likelihood index.

Several spectral methods, developed for hyperspectral data, can be applied to multispectral data such as ASTER. These methods require atmospherically corrected reflectivity images as input. These methods compare the image spectrum of each pixel to spectra measured in the laboratory and assign a likelihood value to each pixel.

3. Study Area

ASTER data have been available to the public since November 2000. Since the ASTER instrument is sharing the Terra spacecraft with a number of other instruments, it is only able to capture approximately 750 scenes each day (an ASTER scene is 60 km square). Although

all images captured are available to the public, specific requests for image capture can only be made by members of the ASTER science team. The long-term objective of the mission is to obtain one-time coverage of the entire land surface. Fortunately, a number of images were acquired over the Atacama Desert late in 2000 (Fig. 1).

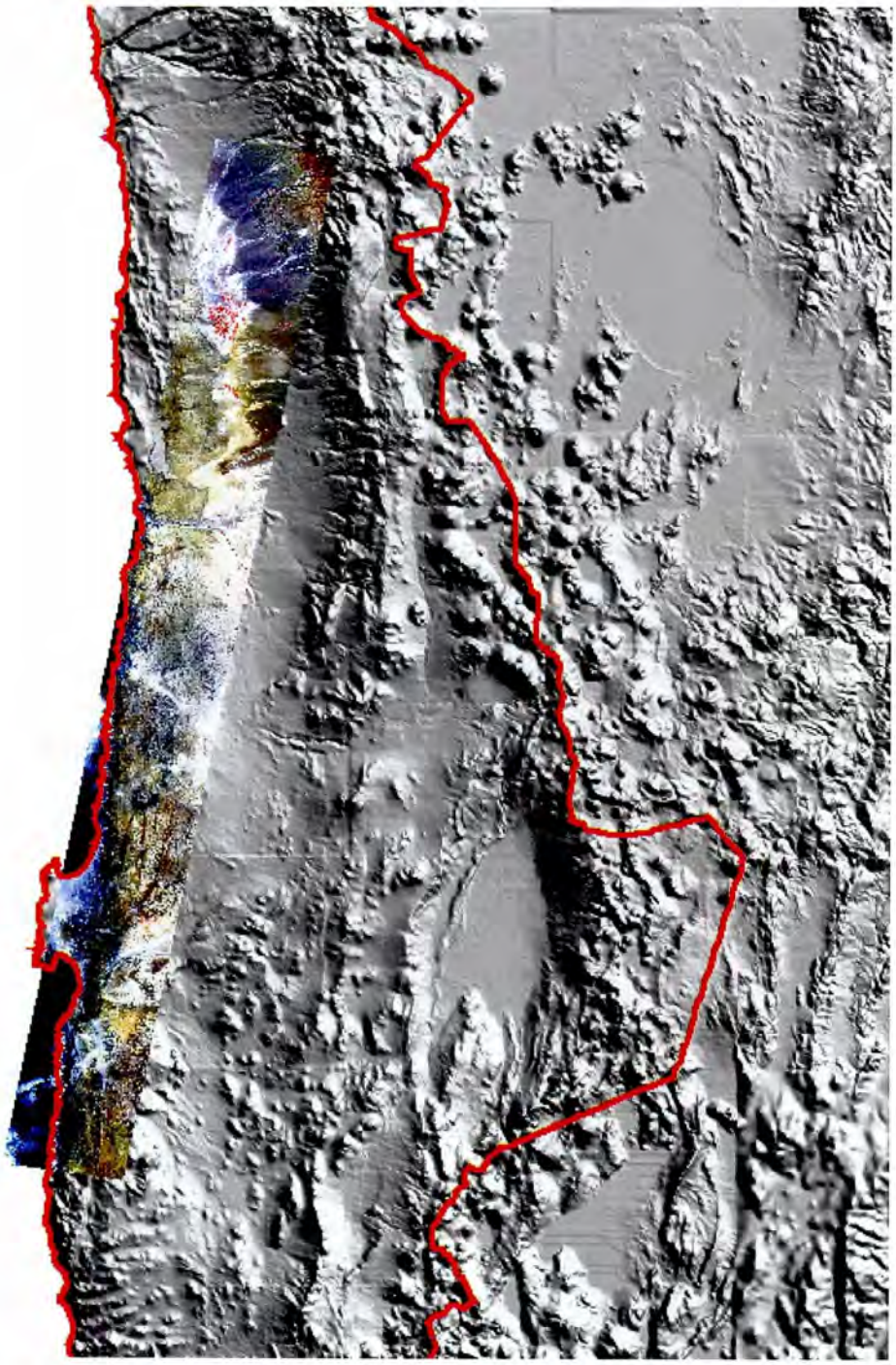

Fig. 1 ASTER scenes acquired October 7, 2000. Shaded relief images is created using GTOPO30 (http://edcdaac.usgs.gov/gtopo30/gtopo30.html). The red line is the Chilean border.

4. Visible Near and Short Wave Infrared Bands

4.1 Results of classification

The three VNIR and six SWIR bands from all the scenes were combined into a single dataset. The isodata classification technique was run until all pixels were assigned one of 50 classes and less than 2% of pixels changed during the last iteration. Since it is impossible to show the results in 9-dimensional space and there are 36 possible band pairs, Fig. 2 shows the results of selected band pairs where the distinction between the classes is most apparent.

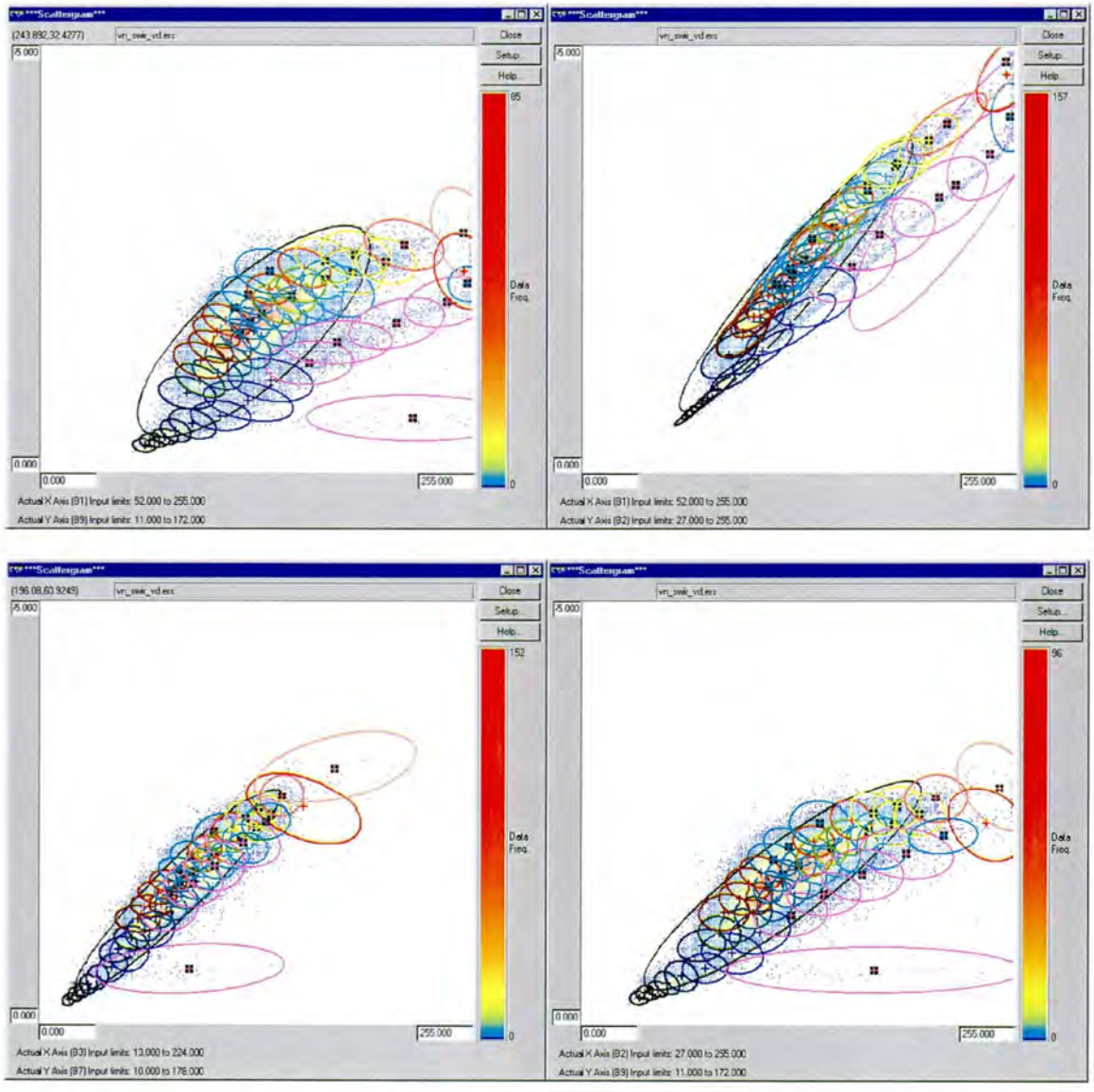

Fig. 2 Scattergrams showing the brightness values of all pixels in the ASTER scene. Each axis shows the value in one band. The means and 95% ellipses are shown for all classes.

The resulting classified image (Plate 1) was displayed beside the original image (Plate 2). Each class was assigned to one of nine groups based upon its geographical distribution.

Fig. 3 shows the average spectrum for each group using all nine bands. The first group makes up 0.38% of the image and is found almost exclusively in storage areas around nitrate

processing plants (Plate 3). This group is considered to represent relatively pure nitrate minerals. The second group (2.69% of the image) is spatially associated with one of the 'nitrate' classes, and is found in very bright areas on the images (Plate 4). This group is tentatively called 'salt' due to its spectral similarity to the 'nitrate' group and its geographic association with salars and nitrate areas. The third group (1.77% of the image) is associated with evaporation ponds at nitrate plants (Plate 5). It is assumed to represent a very wet salty material. In addition to the evaporation ponds, this group is also found along sandy areas of the coast and locally along riverbanks. A fourth group (Plate 6), also found in some evaporation ponds, also occurs over much of the image (26.49%). It is referred to as 'pond-like' in the figures. The fifth group is water (mostly seawater) and makes up 8.54% of the image. The last four groups are unidentified and only called groups 1-4 on the figures. They make up 18.84%, 15.77%, 19.18% and 6.34% of the image respectively. Group 1 (Plate 7) is found in elevated areas and appears to be some type of bedrock. Group 2 (Plate 8) makes up most of the areas identified as salars. Group 3 (Plate 9) is not found in the salars and appears to comprise much of the alluvial material. Group 4 (Plate 10) is restricted to areas near the coast, and appears to be bedrock.

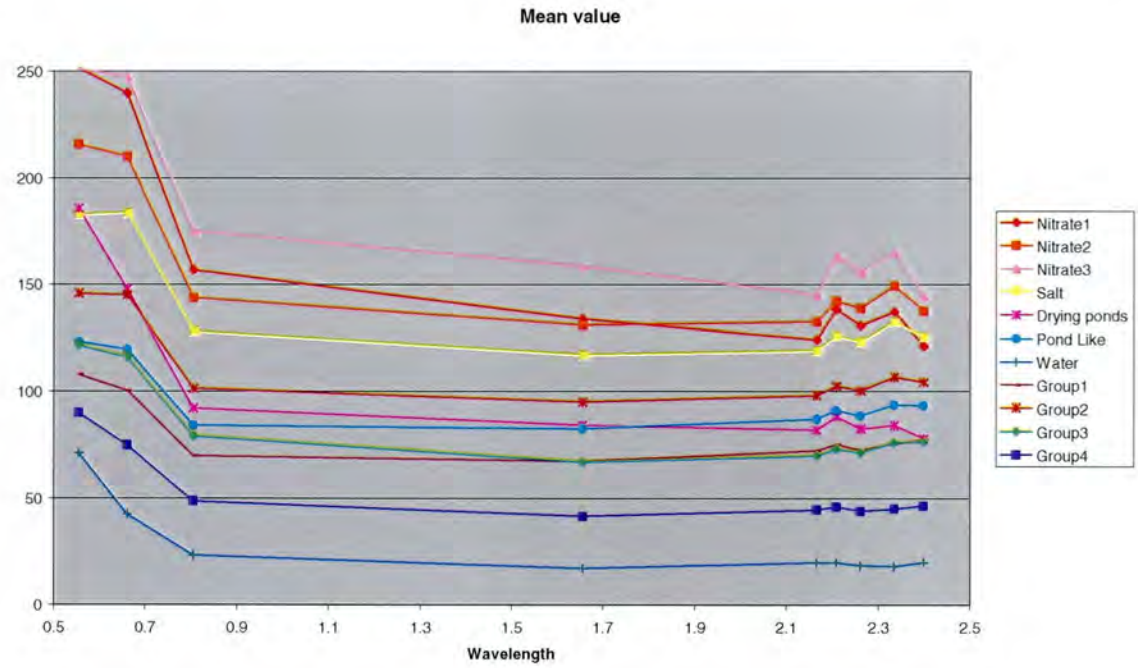

Fig. 3 Average spectra of each group (the 'nitrate' group is divided into its individual classes).

4.2 Spatial correlation of classes with areas of nitrate deposits

Without detailed geological maps, it is impossible to accurately assess what type of material each class represents. Ericksen (1983) presents several figures outlining areas of nitrate fields and salars. While these figures are somewhat crude, they do highlight a correlation between some identified classes and areas of historic nitrate production. In each of the figures in this section, the left image shows an area from one of Ericksen's figures, while the right image shows the classified image for the identical area. Fig. 4 is an index map of Chile showing the location of nitrate deposits and salars in northern Chile.

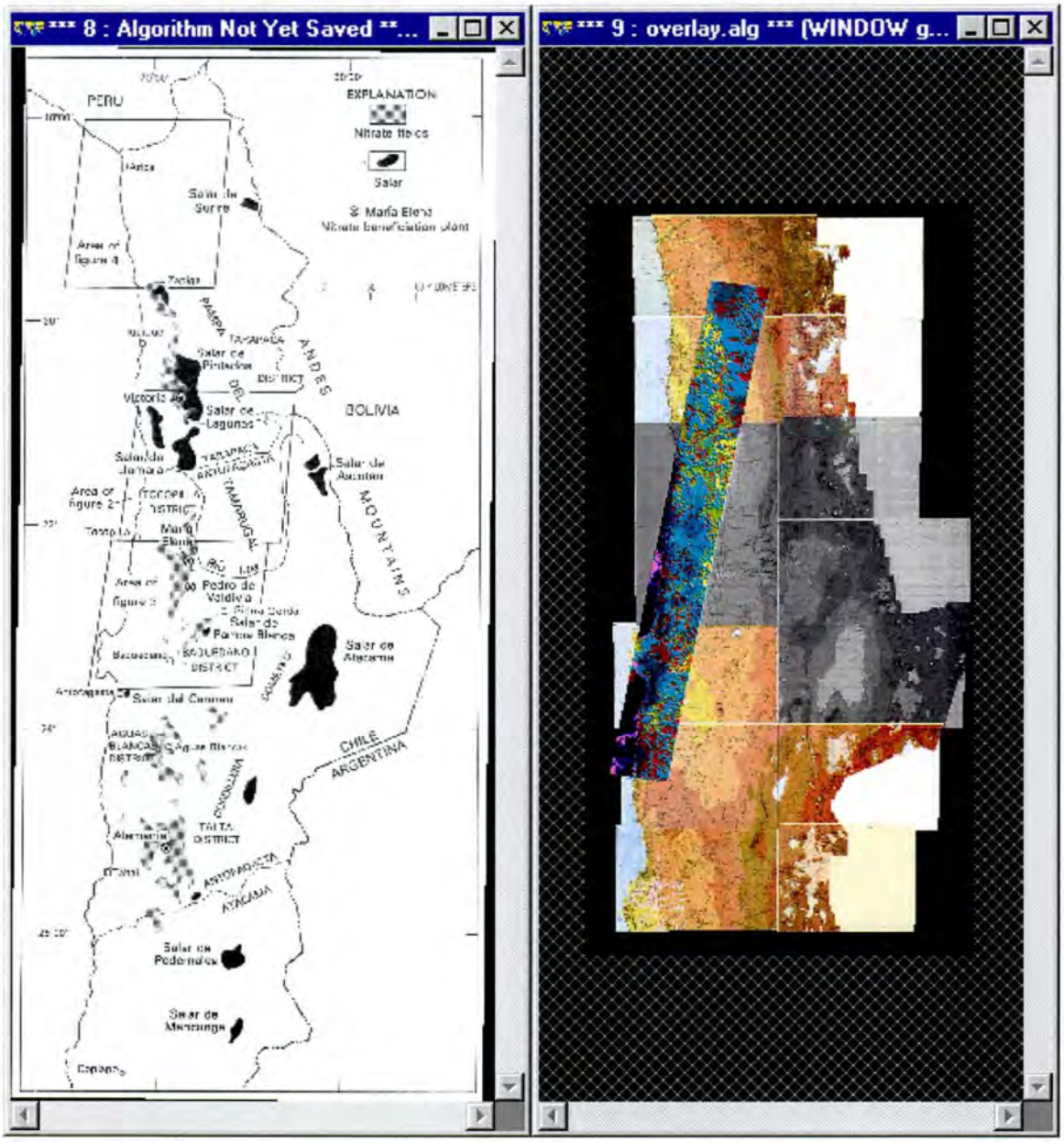

Fig. 4 Figure 1 from Ericksen (1983), showing the location of nitrate deposits and salars. The image on the right is at the same scale and shows the location of the ASTER scenes evaluated for this report.

Figs. 5 and 6 show the northern Tarapacá district, where deposits along the eastern margin of the Coastal Range have been worked since the early 19th century. These deposits contain the richest nitrate ore in northern Chile (Ericksen 1983). There is a clear correlation between the historic nitrate deposits and the areas of 'nitrate' and 'salt' in the classified image.

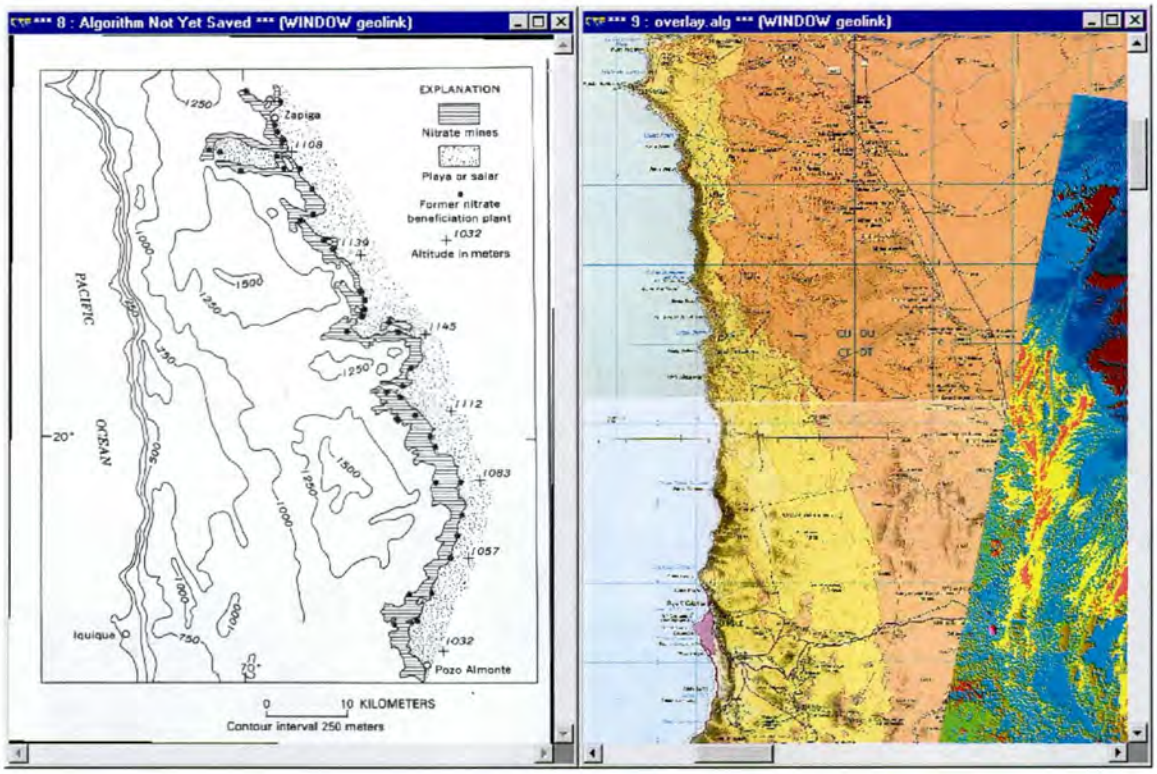

Fig. 5 Figure 8 from Ericksen (1983), showing the historic mining areas along the eastern margin of the Coastal Range in northern Tarapacá district.

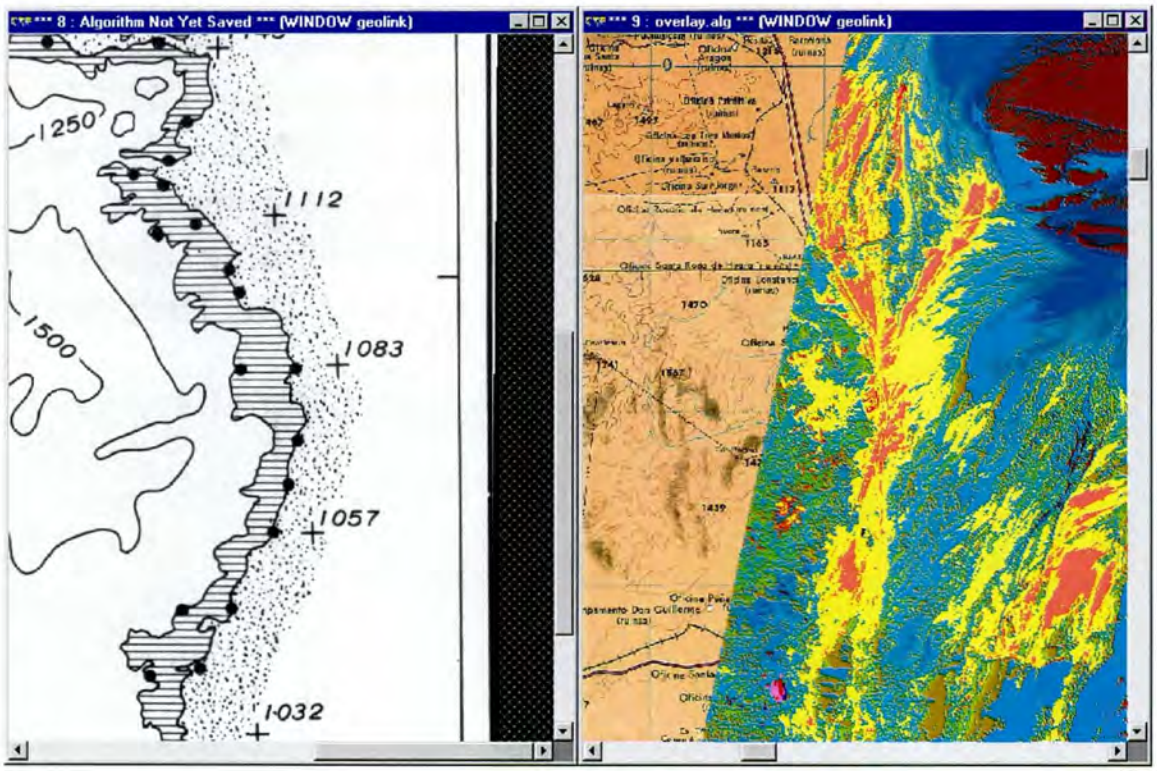

Fig. 6 Closeup of Fig. 5. Note the correlation between the worked nitrate deposits and the 'nitrate' and 'salt' classes in the classified image (pink and yellow colours).

Fig. 7 shows a section of a Landsat image with the principal nitrate workings in the Tocopilla and Baquedano districts. These areas are outlined in red on the classified image, and correlate with areas of 'salt.'

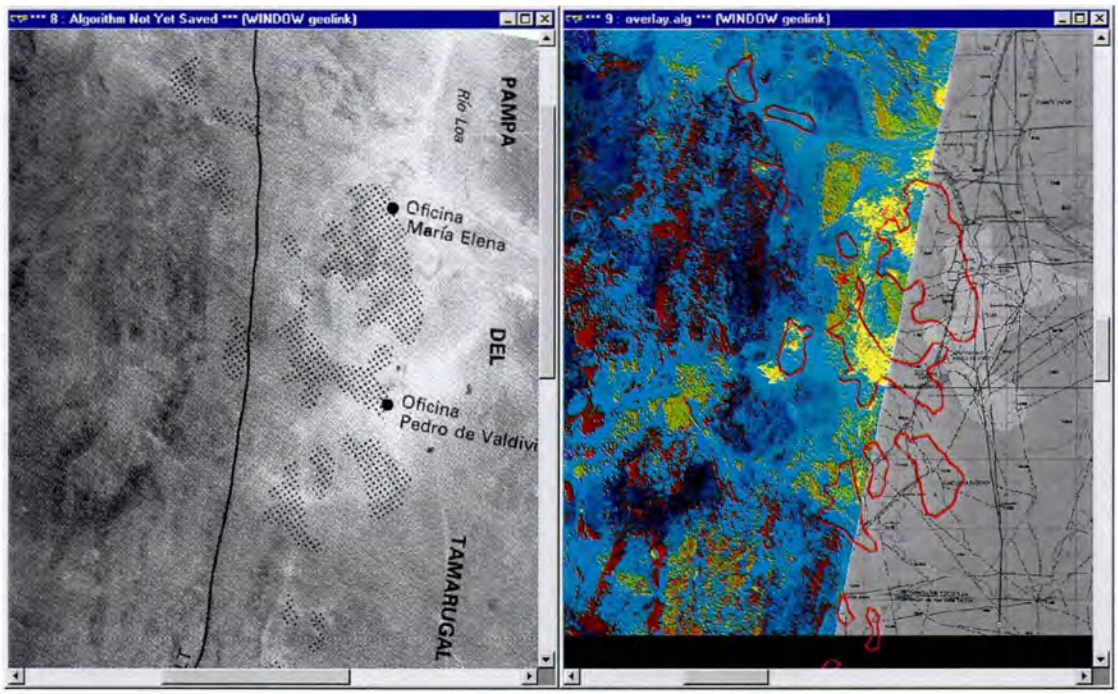

Fig. 7 A portion of Figure 3 from Ericksen (1983) showing the principal nitrate workings in the Tocopilla and Baquedano districts.

Figs. 8 and 9 show sections of a Landsat image in the southern Tarapacá Province. Salar de Llamara and Salar de Bellavista are characterized by classes in Group 2. Classes in the 'salt' and 'nitrate' groups are found nearby.

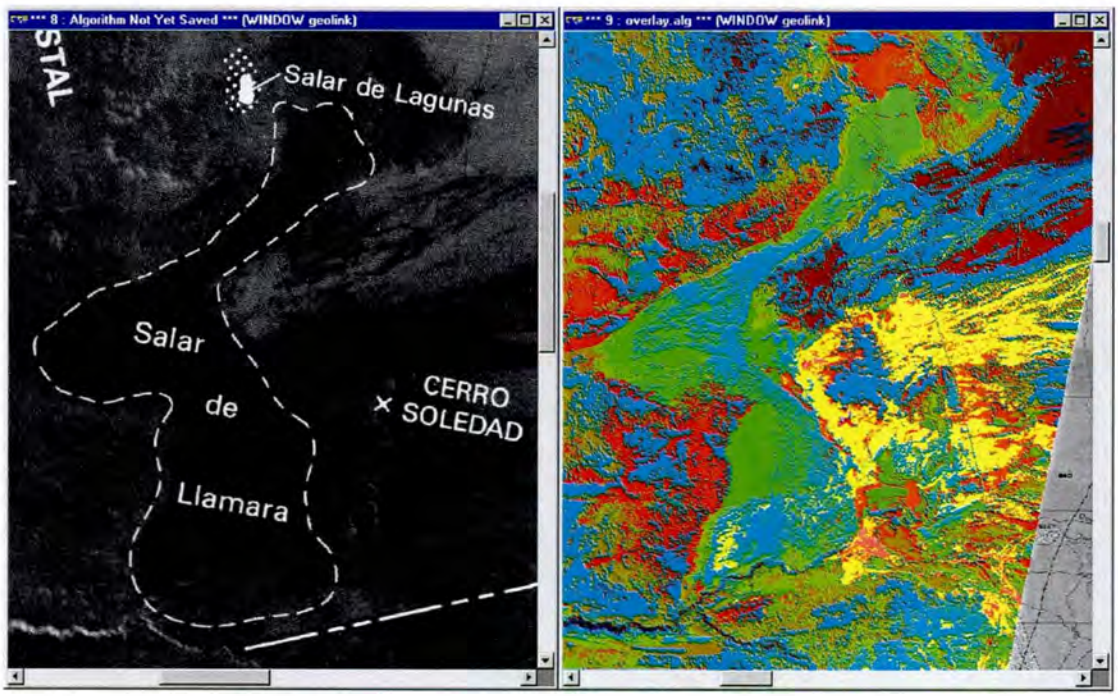

Fig. 8 Portion of Figure 2 from Ericksen (1983) showing Salar de Llamara in the southern Tarapacá Province.

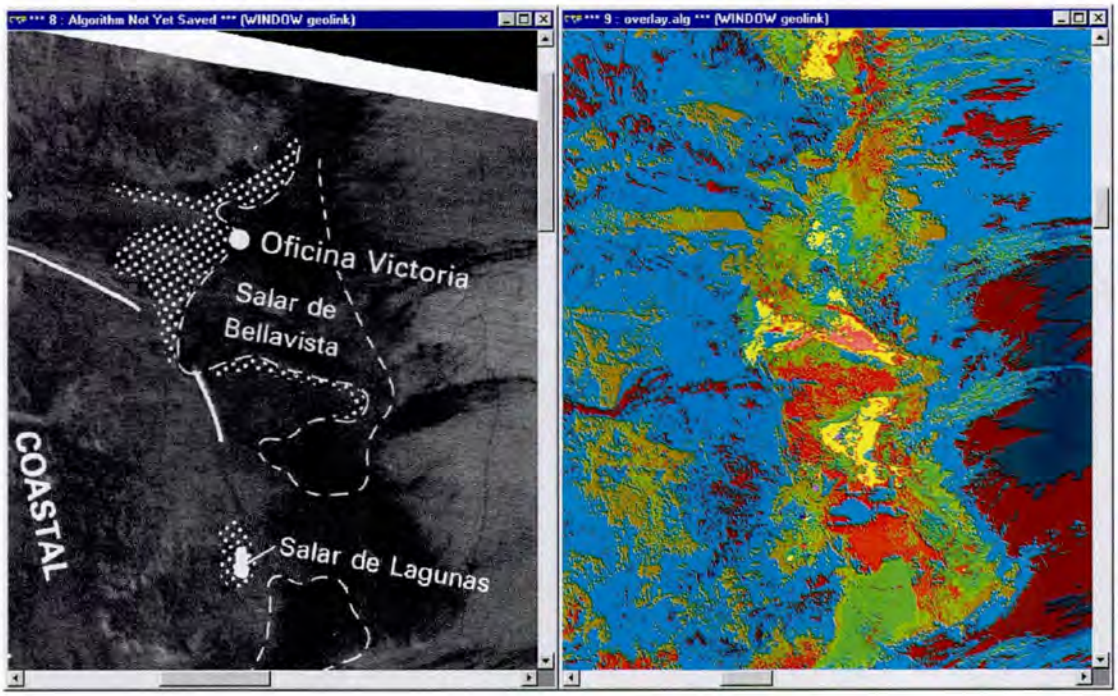

Fig. 9 Portion of Figure 2 from Ericksen (1983) showing Salar de Bellavista in the southern Tarapacá Province.

5. Thermal Infrared Bands

Attempts at classification of raw thermal data from ASTER were not successful. Atmospheric correction and extraction of emissivity is necessary before this data can be used. TIR data can be useful in discriminating between some evaporite minerals (Crowley & Hook 1996), however the 90 metre pixel size of ASTER TIR images may prove to be too coarse to be of use. Further investigation will be done once emissivity data is available.

6. Conclusions and Recommendations for Further Work

While remote sensing provides a valuable means of assessing large land areas, and should always be done before initial fieldwork, the results are highly dependant upon accurate knowledge of at least part of the study area. The lack of available geological maps for the study area makes it difficult to draw firm conclusions about the nature of the materials that each class represents. The ability of the purely statistical analysis of the ASTER data to produce a map that correlates with known areas of nitrate production is promising. At this point, however, it is not possible to translate these results to Namibia. In order to produce a diagnostic signature useful for identification of exploration targets in the Namib Desert, the following must be done:

- Acquire atmospherically corrected data. This is necessary to be able to compare image spectra with those measured in the lab. This data is currently being acquired and will be ready for the next phase of this project if it proceeds.

- Identify training regions. Areas of known geology must be identified, from which the ASTER data can be used to extrapolate. This probably requires opening contact with

Chile to obtain geological maps covering the imaged area. Visits to key areas identified on the images would also be invaluable in interpreting the results of the classification.

- Obtain reference spectra of surface material. Two samples of nitrate ore are presently being measured by Dr. Simon Hook at NASA's Jet Propulsion Laboratory. These samples do not represent surface materials as the main caliche layer occurs 0.5-1 metres below the surface. Measurements of surface materials are necessary to do a proper spectral analysis of the atmospherically corrected data. Ideally a portable spectrometer would be taken to the field to take average measurements over an area, rather that a single rock or soil sample.

The results of this preliminary study are promising and suggest that further study will lead to the identification of nitrate deposits in Chile. That these materials could be found in Namibia is still speculative. However, considering the low cost of the method, there is little to be lost in completing the investigation.

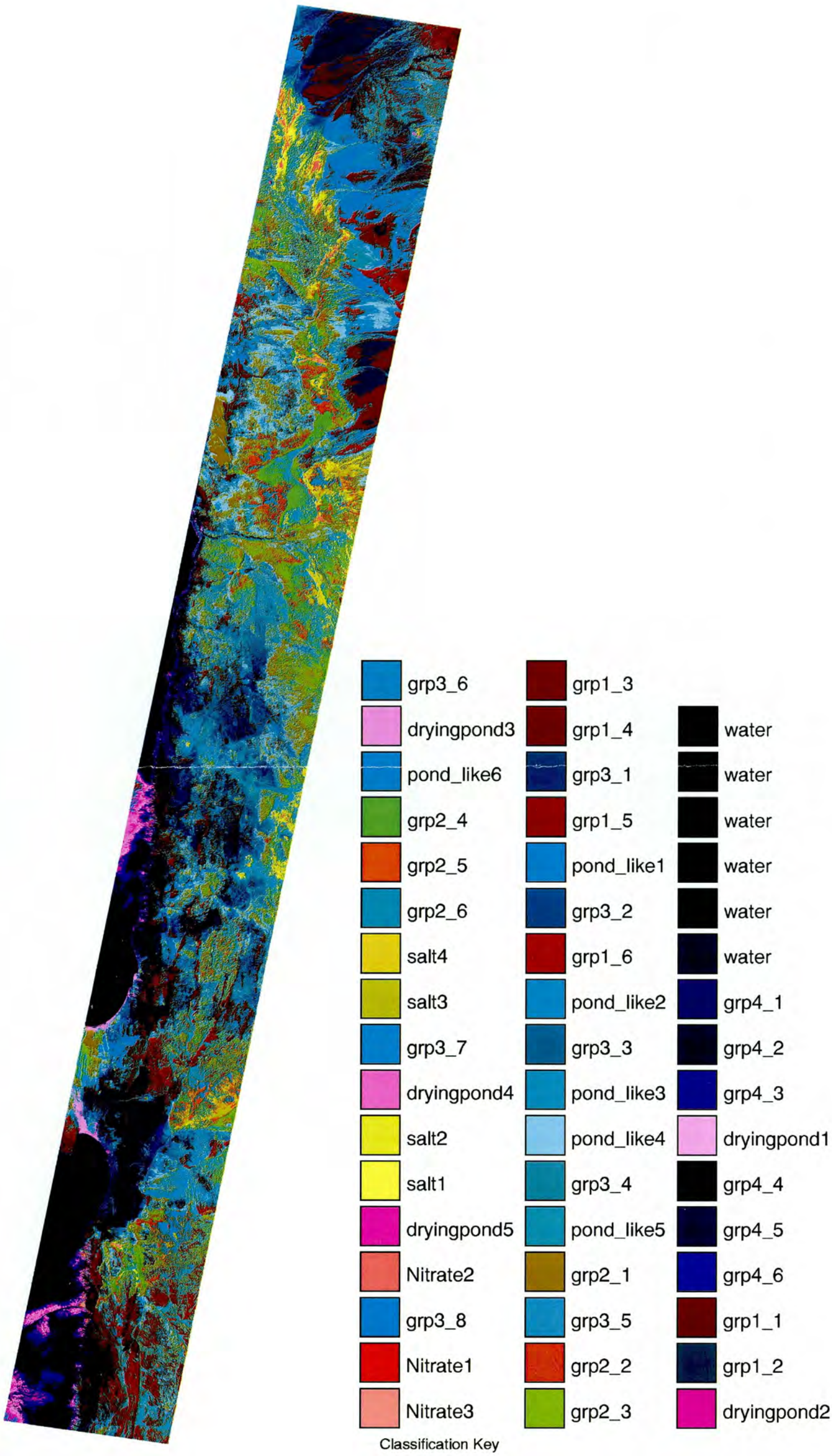

Plate 1 Results of Isoclass unsupervised classification of VNIR and SWIR ASTER bands.

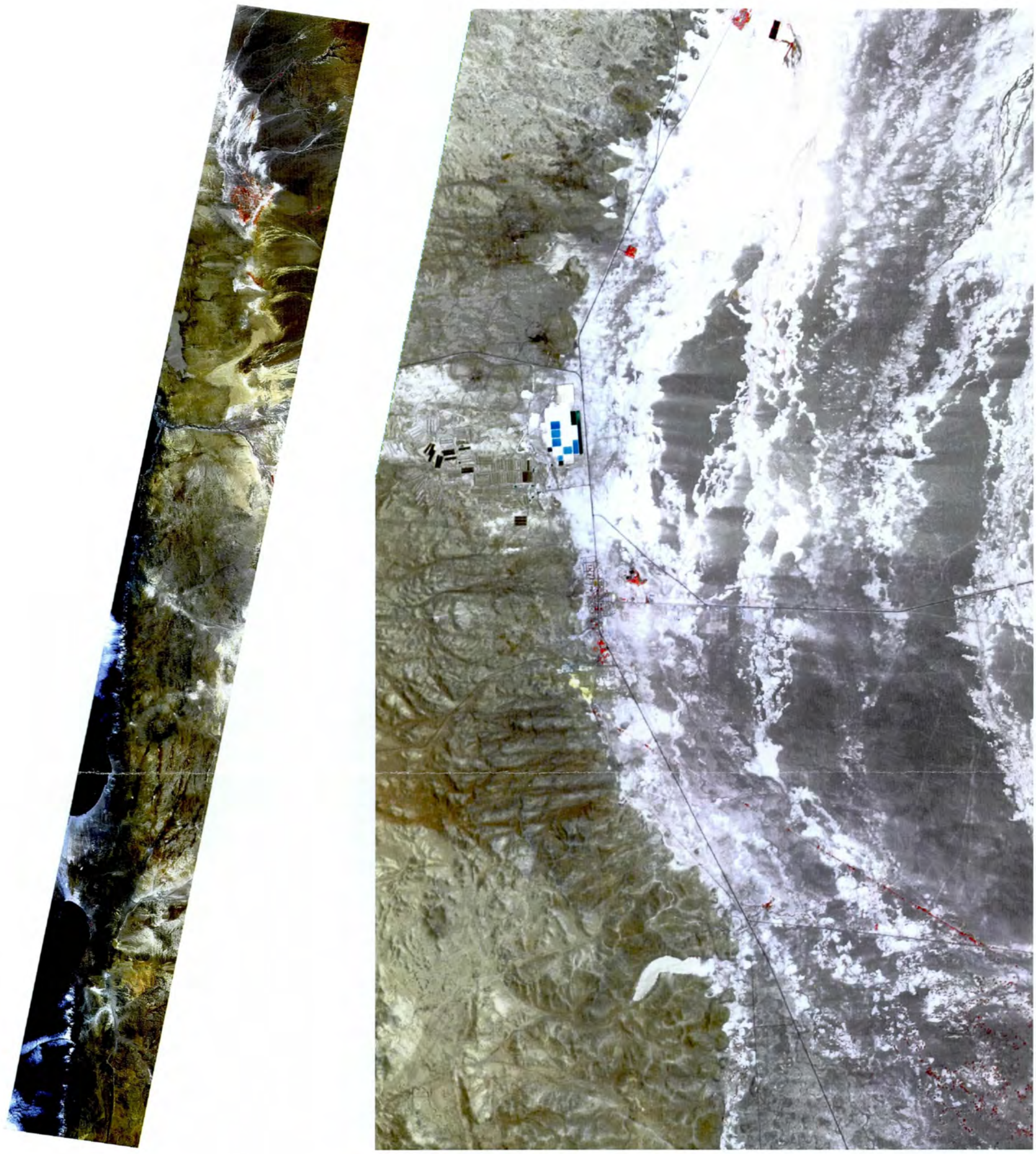

Plate 2 ASTER bands 3, 2 and 1 as red, green and blue. Left image is the full dataset. Right image is from the northwest section and is 15 km wide.

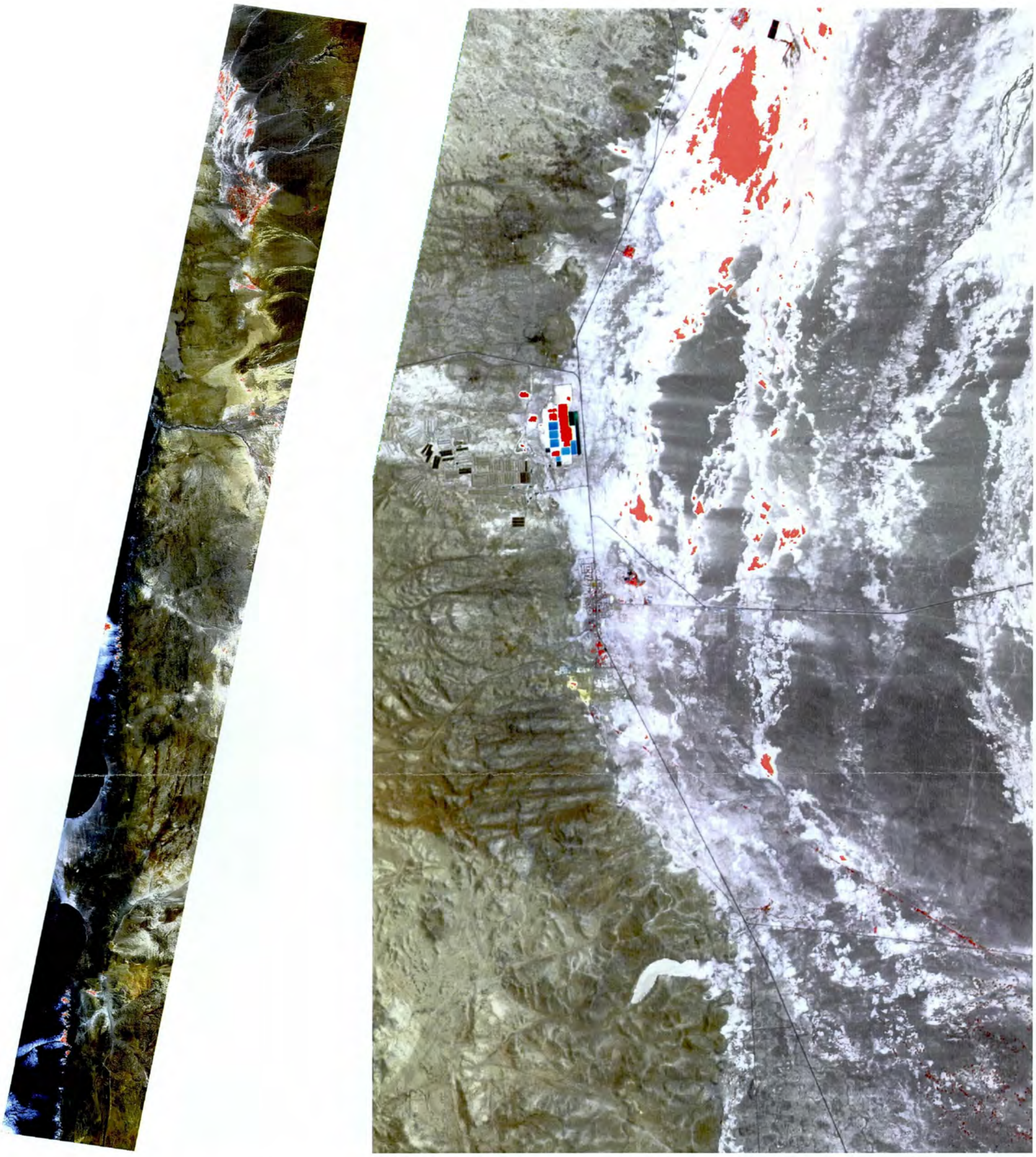

Plate 3 Nitrate classes displayed over ASTER bands 3, 2 and 1. Left image is the full dataset. Right image is from the northwest section and is 15 km wide.

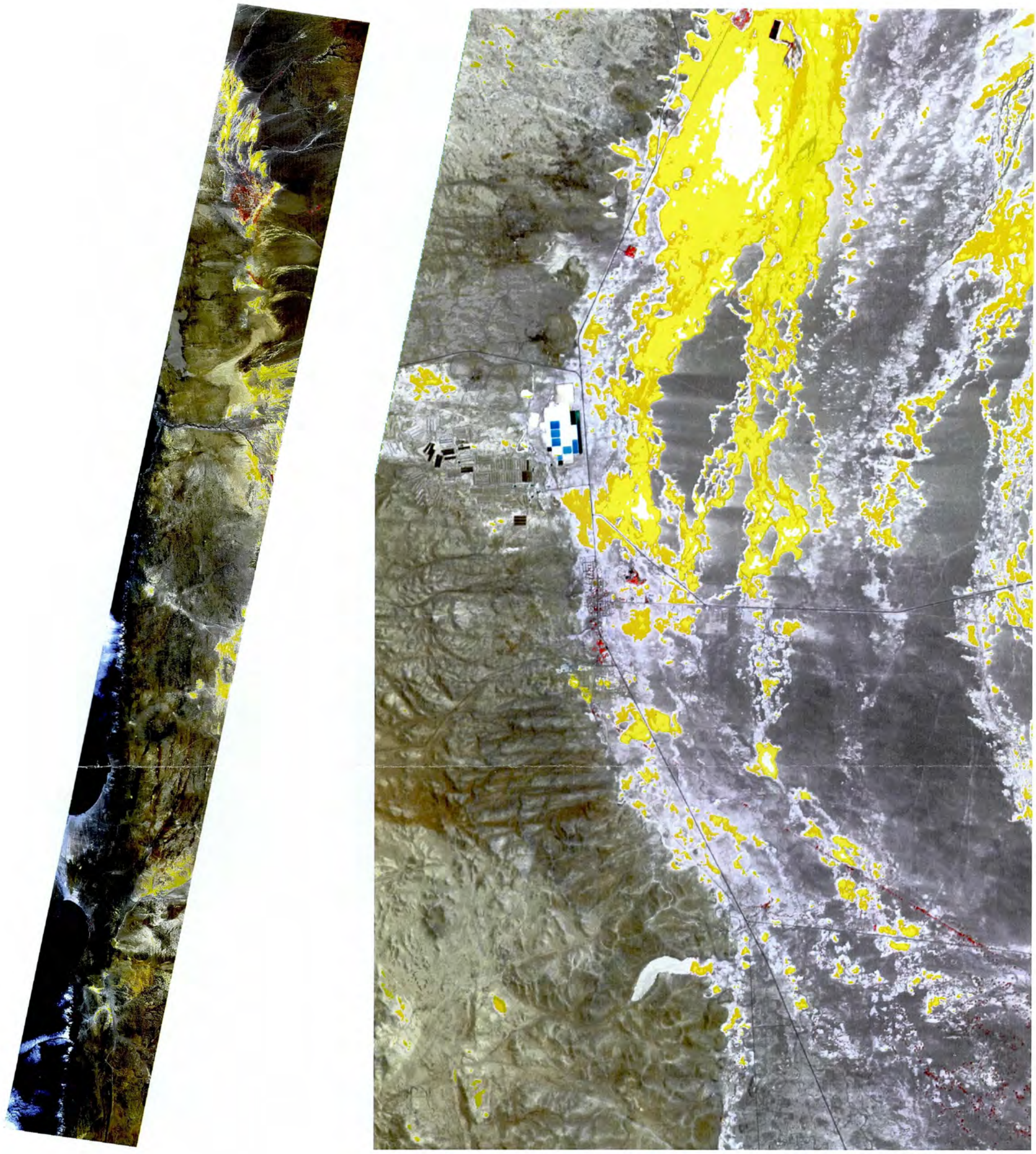

Plate 4 'Salt' classes displayed over ASTER bands 3, 2 and 1. Left image is the full dataset. Right image is from the northwest section and is 15 km wide.

Plate 5 'Drying pond' classes displayed over ASTER bands 3, 2 and 1. Left image is the full dataset. Right image is from the northwest section and is 15 km wide.

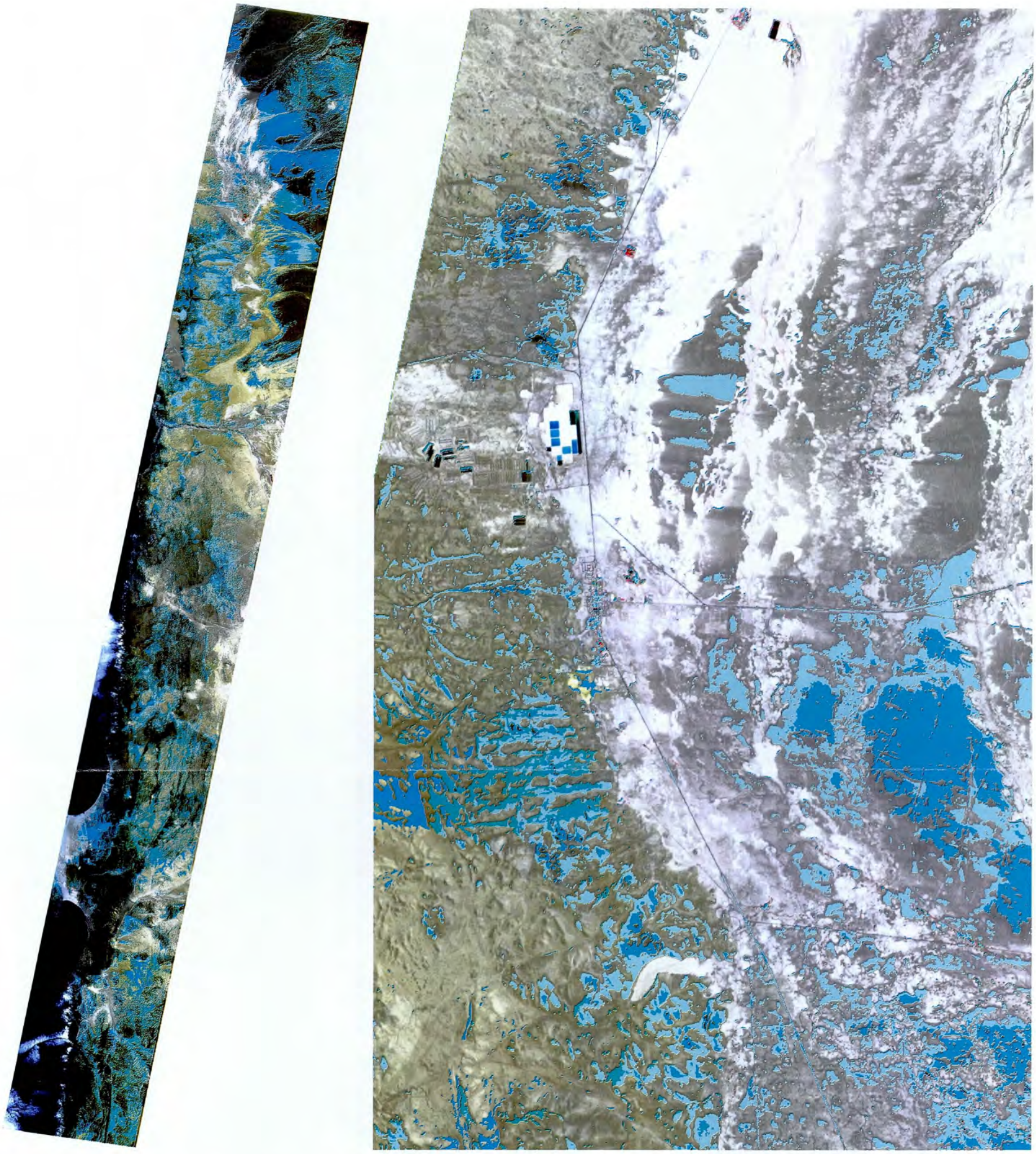

Plate 6 Pond-like classes displayed over ASTER bands 3, 2 and 1. Left image is the full dataset. Right image is from the northwest section and is 15 km wide.

Plate 7 Group1 classes displayed over ASTER bands 3, 2 and 1. Left image is the full dataset. Right image is from the southwest section and is 15 km wide.

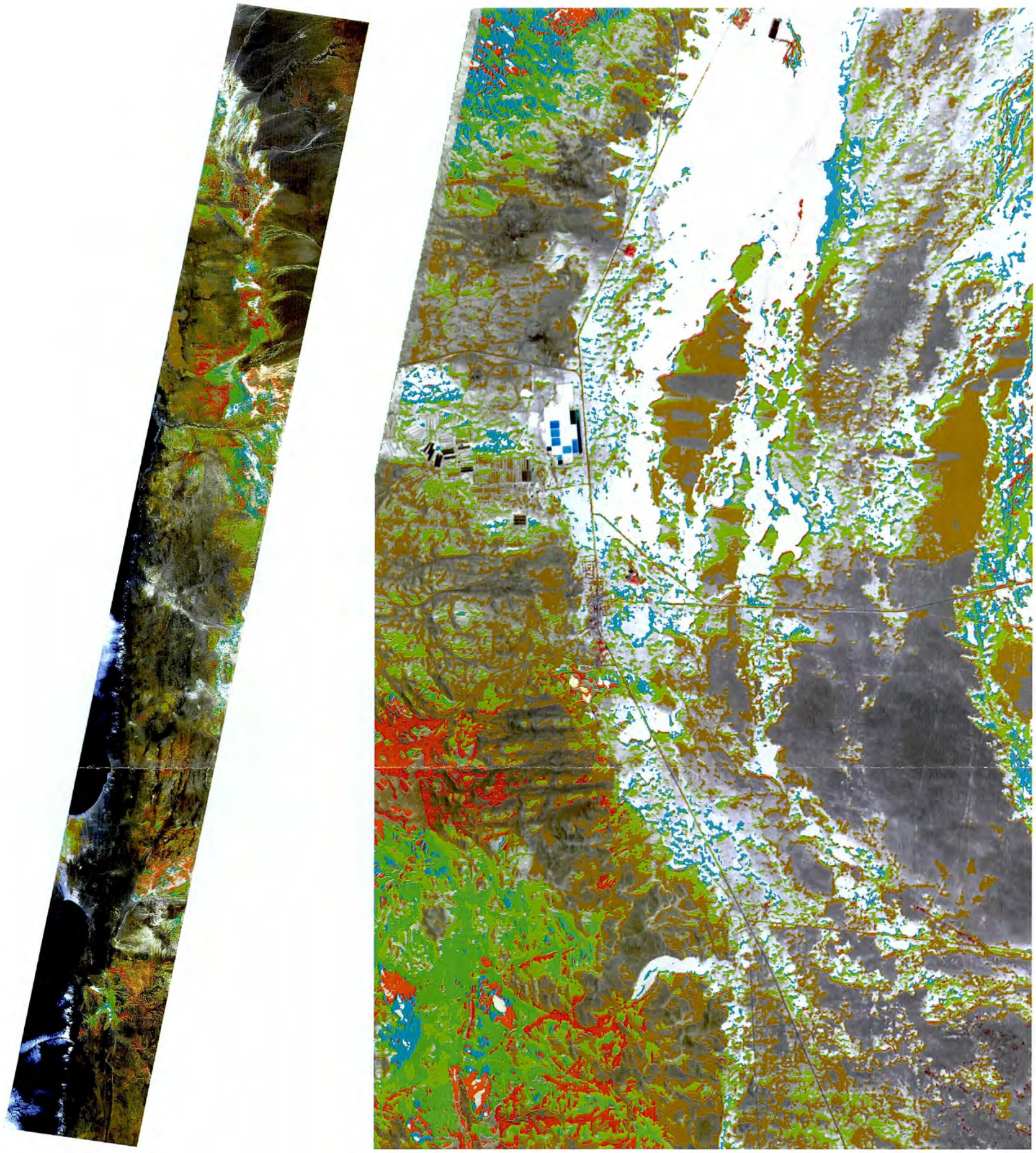

Plate 8 Group 2 classes displayed over ASTER bands 3, 2 and 1. Left image is the full dataset. Right image is from the northwest section and is 15 km wide.

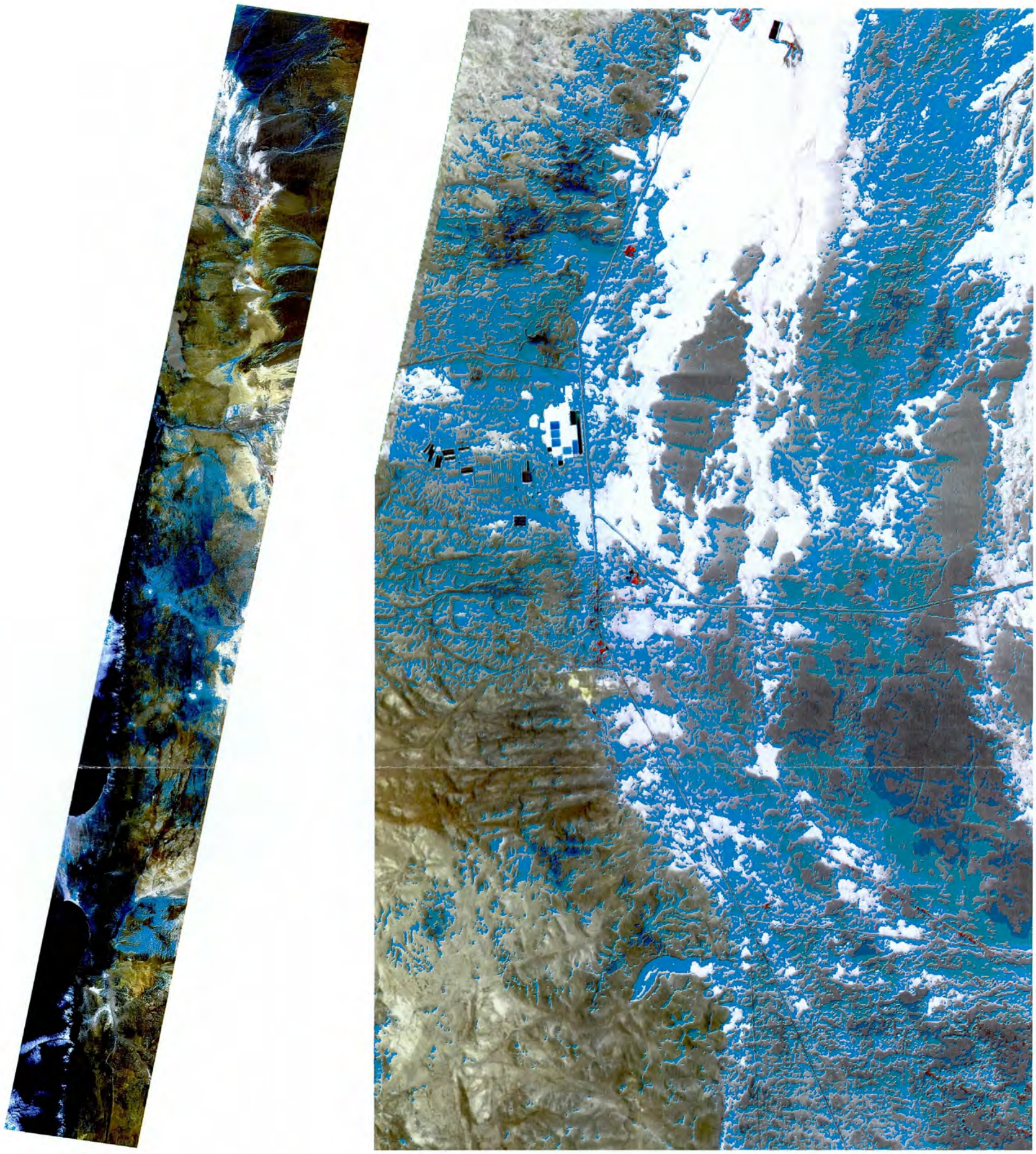

Plate 9 Group 3 classes displayed over ASTER bands 3, 2 and 1. Left image is the full dataset. Right image is from the northwest section and is 15 km wide.

Plate 10 Group 4 classes displayed over ASTER bands 3, 2 and 1. Left image is the full dataset. Right image is from the southwest section and is 15 km wide.

7. References

Böhlke, J. K., Ericksen, G. E. & Revesz, K. 1997. Stable isotope evidence for an atmospheric origin of desert nitrate deposits in northern Chile and Southern California, U.S.A. *Chemical Geology* **136**, 135-152.

Crowley, J. K. & Hook, S. J. 1996. Mapping playa evaporite minerals and associated sediments in Death Valley, California, with multispectral thermal infrared images. *Journal of Geophysical Research* **101**(B1), 643-660.

Ericksen, G. E. 1983. The Chilean nitrate deposits. *American Scientist* **71**(4), 366-374.

Hook, S. J., Gabell, A. R., Green, A. A. & Kealy, P. S. 1992. A comparison of techniques for extracting emissivity information from thermal infrared data for geologic studies. *Remote Sensing of the Environment* **42**, 123-135.